ARTICLE
Journal of Cellular Biochemistry 113:19–30 (2012)

Journal of Cellular Biochemistry

A Simple and Economical Route to Generate Functional Hepatocyte-Like Cells From hESCs and Their Application in Evaluating Alcohol Induced Liver Damage

Rajarshi Pal,[1] Murali Krishna Mamidi,[2] Anjan Kumar Das,[2] Pawan Kumar Gupta,[1] and Ramesh Bhonde[1*]

[1] *Manipal Institute of Regenerative Medicine, Manipal University Branch Campus, # 10 Service Road, Domlur Layout, Bangalore 560071, India*

[2] *Stempeutics Research Malaysia Sdn. Bhd, Enterprise 4, Technology Park Malaysia, Bukit Jalil, 57000 Kuala Lumpur, Malaysia*

ABSTRACT

The in vitro derived hepatocytes from human embryonic stem cells (hESC) is a promising tool to acquire improved knowledge of the cellular and molecular events underlying early human liver development under physiological and pathological conditions. Here we report a simple two-step protocol employing conditioned medium (CM) from human hepatocellular carcinoma cell line, HepG2 to generate functional hepatocyte-like cells from hESC. Immunocytochemistry, flow cytometry, quantitative RT-PCR, and biochemical analyses revealed that the endodermal progenitors appeared as pockets in culture, and the cascade of genes associated with the formation of definitive endoderm (HNF-3β, SOX-17, DLX-5, CXCR4) was consistent and in concurrence with the up-regulation of the markers for hepatic progenitors [alpha-feto protein (AFP), HNF-4α, CK-19, albumin, alpha-1-antitrypsin (AAT)], followed by maturation into functional hepatocytes [tyrosine transferase (TAT), tryptophan-2, 3-dioxygenase (TDO), glucose 6-phosphate (G6P), CYP3A4, CYP7A1]. We witnessed that the gene expression profile during this differentiation process recapitulated in vivo liver development demonstrating a gradual down-regulation of extra embryonic endodermal markers (SOX-7, HNF-1β, SNAIL-1, LAMININ-1, CDX2), and the generated hepatic cells performed multiple liver functions. Since prenatal alcohol exposure is known to provoke irreversible abnormalities in the fetal cells and developing tissues, we exposed in vitro generated hepatocytes to ethanol (EtOH) and found that EtOH treatment not only impairs the survival and proliferation, but also induces apoptosis and perturbs differentiation of progenitor cells into hepatocytes. This disruption was accompanied by alterations in the expression of genes and proteins involved in hepatogenesis. Our results provide new insights into the wider range of destruction caused by alcohol on the dynamic process of liver organogenesis. J. Cell. Biochem. 113: 19–30, 2012.

KEY WORDS: HUMAN EMBRYONIC STEM CELLS; LIVER ORGANOGENESIS; DEFINITIVE ENDODERM; HEPATOCYTE-LIKE CELLS; CONDITIONED MEDIUM; ALCOHOL; LIVER TOXICITY

The liver is the major organ for metabolism and detoxification in the human body, which justifies the ongoing research to identify a reliable source of functional hepatocyte-like cell types for in vitro testing. Till date the complexity and function of the liver could not be replicated by any available in vitro cell type or cell-based model [Elaut et al., 2006; Guillouzo et al., 2007; Tuschl et al., 2008]. The availability of human primary liver cells is not only limited but also these cells lose their normal phenotype and functional properties when used in vitro. Transformed hepatic cell lines contain very low levels of drug metabolizing enzymes and have substantially aberrant expression profiles of other important proteins from the native hepatocyte in vivo. Thus, many tests of drug metabolism and toxicity are still performed using animal models, even though liver metabolism is known to be species-specific [Greer et al., 2010; Manna et al., 2010]. Since none of the existing models are able to recreate the dynamic process of hepatogenesis [Zorn and Wells, 2009], there is an urgent need for a suitable in vitro model that mimics human liver development and therefore can be used for the evaluation of stage-specific effect of toxicants.

The dynamic processes involved in liver development are orchestrated by subtle up- and/or down-regulation of certain characteristic genes representing early, middle, and later stages of cellular development thus acting as molecular switches [Gualdi

Additional supporting information may be found in the online version of this article.

*Correspondence to: Ramesh Bhonde, Manipal Institute of Regenerative Medicine, Manipal University Branch Campus, # 10 Service Road, Domlur Layout, Bangalore 560071, India. E-mail: rr.bhonde@manipal.edu

Received 17 September 2011; Accepted 21 September 2011 • DOI 10.1002/jcb.23391 • © 2011 Wiley Periodicals, Inc.
Published online 28 September 2011 in Wiley Online Library (wileyonlinelibrary.com).

et al., 1996; Zaret et al., 2008]. Sufficient evidence is now available to support the formation of metabolically active hepatocytes [Barr and Streissguth, 2001; Rambhatla et al., 2003; Shirahashi et al., 2004; Schwartz et al., 2005; Cai et al., 2007; Duan et al., 2007; Hay et al., 2008a; Basma et al., 2009] from human embryonic stem cells (hESCs) in response to appropriate developmental cues, a process which closely mimics in vivo liver formation.

Alcohol consumption during pregnancy often results in abnormal fetal development (fetal alcohol syndrome; FAS) leading to anatomical and behavioral defects collectively known as fetal alcohol spectrum disorders (FASD). In general, ethanol (EtOH) has been implicated with induction of apoptosis, inhibition of proliferation, differentiation, migration, and other cellular functions [Miller et al., 1990; Baroni et al., 1994; Li et al., 2001; Young et al., 2003; Siegenthaler and Miller, 2004]. Experimental evidence further demonstrates that EtOH interferes with many ontogenic phases of brain [Guan et al., 2004], liver [Cartwrigh et al., 1998], and heart [Dunty et al., 2001] development during embryogenesis. Moreover, it is well known that alcohol consumption causes excessive apoptosis or oxidative stress in early embryos, thereby leading to an abnormal phenotype.

In the present study we report for the first time, that feeder-free adherent cultures of hESC in presence of conditioned medium (CM) from the human hepatocellular carcinoma cell line, HepG2 in a simplified two-step protocol gives rise to definitive endoderm cells followed by preferential conversion into hepatic progenitors and subsequent maturation to functional hepatocyte-like cells. Since the process of liver development depends on the addition of appropriate stage and tissue specific growth factors and supplements [Shirahashi et al., 2004; Kang et al., 2009; Brolen et al., 2010], we hypothesized that the addition of HepG2-CM could promote the maturation and functionality of these putative hepatic progenitors [Hay et al., 2008b]. Molecular and proteomic analyses of these hESC-derivatives revealed expression of stage-specific expression of key markers and functional activity. Further, we investigated the vulnerability of these cultures to EtOH treatment at different stages of differentiation. We demonstrate that EtOH, at physiological relevant concentrations, impairs cell survival and affects the differentiation of hESCs into hepatocyte-like cells by altering their gene and protein expression patterns and functional activity. Our results provide new insights toward a better understanding of early liver organogenesis during normal and perturbed development.

MATERIALS AND METHODS

hESC CULTURE

Continuous cultures of HUES-7 and HUES-9 cell lines were grown on 0.2% gelatin-coated, mitomycin C (Sigma; 10 μg/ml) inactivated mouse embryonic fibroblast (MEF) feeders in a standard ES-cell culture medium consisting of 80% KO-DMEM (Invitrogen), 15% ES-tested FBS (Hyclone), 5% serum replacement (SR, Invitrogen), 1% non-essential amino-acid solution (Invitrogen), 1 mM glutamine (Invitrogen), 0.1% β-mercaptoethanol (Sigma), 4 ng/ml human basic fibroblast growth factor (bFGF; Sigma). Media was replenished every day with pre-equilibrated for 2 h at 37°C and 5% CO_2 incubator and manual passaging was done on every 5th day using the sharp edge of a flame-pulled Pasteur pipette under the stereomicroscope (Olympus; SZX16). The cultures were maintained at 37°C and 5% CO_2 in air (Binder, Camarillo, CA) and used for characterization and differentiation studies. MEF feeders were cultured in DMEM high glucose (Invitrogen) supplemented with 10% fetal bovine serum (FBS; Hyclone), 2 mM glutamine, and 1% non-essential amino acids (Invitrogen).

DIFFERENTIATION PROTOCOL

EMBRYOID BODY (EB) FORMATION

Formation of EBs was induced by mechanical dissociation of undifferentiated hES colonies into pieces less than 200 μm in size using the sharp edge of a flame-pulled Pasteur pipette under the stereomicroscope. These pieces were transferred to 60-mm sterile petri dishes (Corning) to allow their aggregation and prevent attachment on to the plate. Equal sized EBs was grown in suspension culture at approximately 30–40 EBs per dish. The EBs were grown in similar culture medium in absence of bFGF for no less than 4 days; media was changed every alternative day.

COLLECTION OF HepG2- CONDITIONED MEDIA (HepG2-CM)

HepG2 liver carcinoma cells (ATCC HB-8065, UK) were cultured to collect the conditioned media (CM). HepG2 cell line was grown in T-75 tissue culture flasks (Nunc) at 37°C in a 5% CO_2 humidified incubator using 20 ml of DMEM (Invitrogen) supplemented with 10% FBS (Hyclone), and 1% penicillin-streptomycin (Invitrogen) at a seeding density of 5.0×10^4 cells/cm^2. Twenty-four hours post seeding, the medium was removed to get rid of the floating cells and fresh medium was added. We collected CM from HepG2 at two different time points which indicates two distinct phases of their growth and development. The first batch of media was collected on day 2 when the cultures were ~40–50% confluent and the second batch was collected on day 4 once the cultures attained ~75–85% confluence. Each time after collecting the culture media, it was centrifuged at 1,500 rpm for 10 min and the supernatant was decanted carefully leaving 1 ml in the centrifuge tube, which was then passed through sterile 0.22 μ (Millipore) filters to ensure cell free media. Every batch of HepG2-CM was stored at −20°C freezer for short-term usage and −80°C freezer for long-term usage.

DEFINITIVE ENDODERM INDUCTION AND HEPATOCYTE MATURATION USING HepG2-CM

A novel two-step protocol was designed with an aim to induce the formation of definitive endoderm cells followed by enrichment of hepatic progenitors and subsequent enhancement of their maturation into functionally active hepatocyte-like cells. HepG2-CM was employed at two stages after onset of differentiation in absence of bFGF.

Via Adherent Cultures of hESC. Feeder-free hESCs were grown on 1% matrigel coated tissue culture plates in normal hESC medium in presence of bFGF. As soon as these cultures attained confluency (4–5 days), bFGF was withdrawn from the media and the adherent

cultures were allowed to differentiate spontaneously up to day 7. Once definitive endoderm formation was observed, day 2 HepG2-CM was added in the ratio of 1:1 (v/v) along with normal EB medium on day 7 and continued for 1 week to enhance the differentiation of hepatic progenitor cells. Then on day 14, we added the day 4 HepG2-CM in the same proportion continuously for another 1 week till 21 days of differentiation. This enabled the maturation of committed progenitor cells into functional hepatocyte-like cells. Following 21 days, the control and experimental groups were further cultured for up to 35 days in normal EB medium without HepG2-CM. The cultures were maintained at 37°C in a 5% CO_2 humidified incubator and fed every 2 days.

ETHANOL TREATMENT

Concentrations of EtOH (Sigma) tested in this study were 5, 20 and 50 mM which corresponds to low dose (LD), medium dose (MD), and high dose (HD), respectively. EtOH was directly diluted in the culture medium to the final test concentrations. We exposed the hepotocyte cultures (day 14–21) to various concentrations of EtOH up to 48 h and examined the effects in comparison to untreated controls (Fig. 4A). Instead of six well plates, separate tissue-culture dishes (35 mm Falcon plates) were used for the treated groups in order to nullify the impact of EtOH vapor irrespective of the concentration.

CELL VIABILITY ASSAY

Cell viability was determined by the 7-amino actinomycin (7-AAD). 7-AAD is a fluorescent DNA intercalator which binds to double stranded DNA of the dead and damaged cells. Following EtOH treatment, cells were washed twice with PBS; 100 μl of the cell suspension consisting of 1×10^5 cells were transferred to a 15 ml centrifuge tube and 5 μl of 7-AAD fluorescent dye was added to each tube. Cells were gently vortexed and incubated for 15 min at room temperature (25°C) in the dark. Cell suspension was subsequently analyzed by flow cytometry (excitation at 488 nm, emission at 520 nm) and appropriate compensation controls were performed in conjunction to establish the gates with the reference

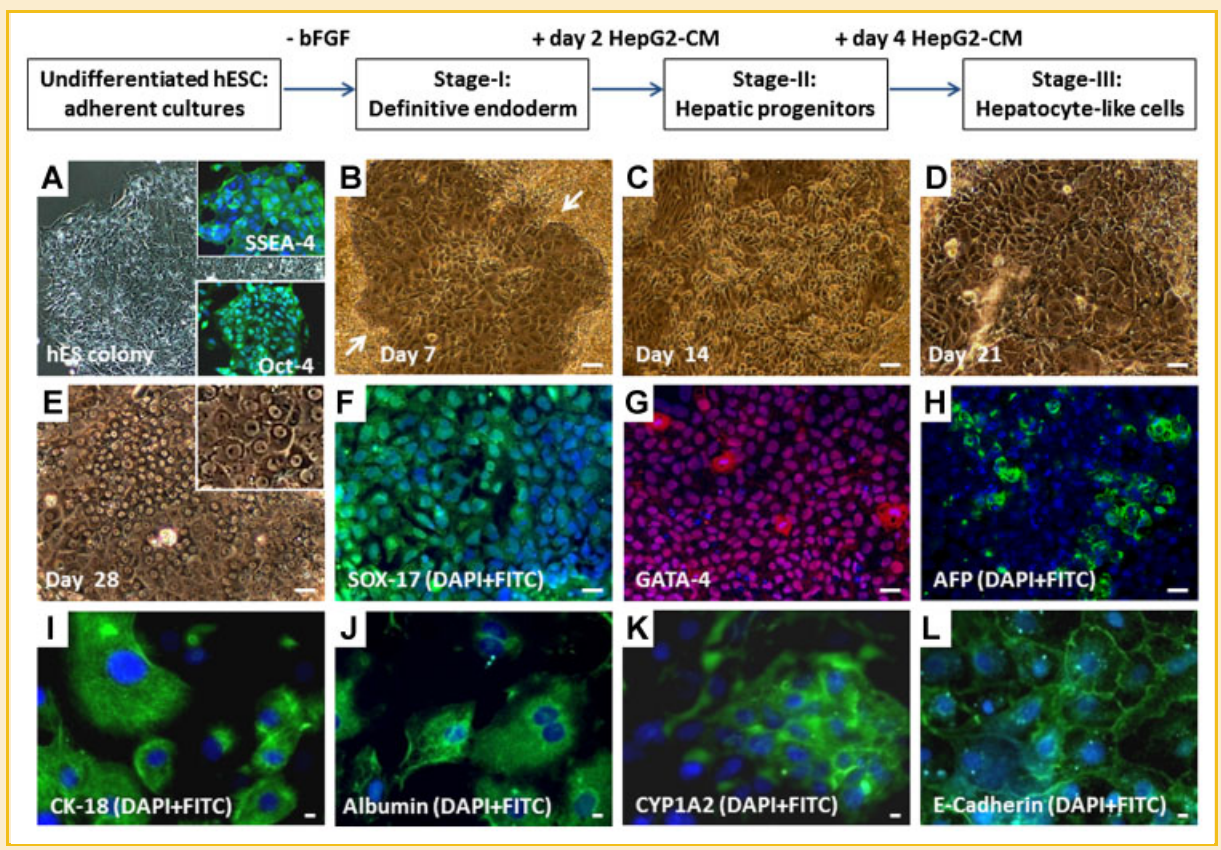

Fig. 1. Guided differentiation of hESC into hepatocyte-like cells: Schematic diagram representing the three-step protocol for hepatic differentiation of hESCs using HepG2-CM. A: Phase contrast photomicrographs of an undifferentiated colony of hESC (HUES-7) grown without feeders; cells demonstrate a typical ES cell-like morphology with clear shining borders. B–E: Images showing sequential change in morphology of undifferentiated cells during progressive days in culture; first toward definitive endoderm (B) followed by hepatic precursor or hepatoblasts (C) and finally into hepatocyte-like cells (D,E). Increase in the number of binucleated, polygonal, epithelial-like cells appearing in pockets was observed with increasing number of days in differentiation. F–L: Immunocytochemical staining shows expression of stage-specific markers during in vitro hepatic differentiation. Majority of the differentiated cells in HepG2-CM induced cultures were positive for SOX-17 (F), GATA-4 (G), AFP (H), CK-18 (I), albumin (J), CYP1A2 (K), and E-Cadherin (L) antibody staining indicating true hepatic characteristics. The blue color represents nuclei counterstained with DAPI while green and red color represents FITC and Rhodamine conjugation, respectively. Negative controls were performed with corresponding immunoglobulin G (IgG). Representative data from one of three experiments are shown ($n = 3$). Scale bar: 100–200 μm.

values. Ten thousand cells were analyzed for each sample and data was acquired using Cytosoft, Version 5.2, Guava Technologies (Millipore).

RNA ISOLATION, cDNA SYNTHESIS AND SEMI-QUANTITATIVE PCR

Cell pellets from control and target groups were collected and total RNA was isolated by the Trizol method (Invitrogen) as per the manufacturer's protocol; RNA was stored at −80°C. The quantity of RNA was checked using a spectrophotometer (Agilent, NanoDrop, Technologies Inc.) and the purity was assessed by determining the 260/280 nm ratio. The first strand of cDNA was synthesized using 1 μg of RNA treated with RNase-OUT ribonuclease inhibitor and Superscript II First Strand Synthesis system (Invitrogen) as per the manufacturer's instructions. PCR reaction for all gene markers (Suppl. Table 1) was performed in 0.2-ml eppendorf tubes (Axygen) with a final volume to 12.5 μl. The amplification program for PCR consisted of an initial denaturation step at 94°C for 5 min, followed by 35 cycles of 30 s denaturing (94°C), 45 s annealing (temperature of the respective gene primer), 45 s elongation (72°C); a final extension at 72°C for 10 min and finally soaking at 4°C. Amplified PCR products were analyzed on 1.5% agarose gel stained with ethidium bromide (EtBr, Sigma), viewed under a UV trans-illuminator, and photographed on a gel documentation system (Pharmacia Biotech, Piscataway, NJ). GAPDH was used as the housekeeping gene and 100-bp ladder (Invitrogen) was used as molecular weight markers.

REAL-TIME QUANTITATIVE (Q)-PCR

The expression of a focused panel of stage specific markers implicated in liver development was performed using SYBR green master mix (Applied Biosystems) in triplicates on an ABI Prism 7900HT Sequence Detection System (Applied Biosystems). The levels of gene expression in hESC grown with HepG2-CM (target) relative to the level of expression in spontaneous cultures (calibrator) was analyzed using the ABI Prism 7900HT Sequence Detection System software (SDS v2.2 software) with the Comparative cycle threshold (Ct) method (ΔΔCt). The primer sequences used in this study are tabulated in Suppl. Table 1. After an initial denaturation for 10 min at 95°C, the reaction was run for 40 cycles of PCR (95°C for 15 s, 60°C for 1 min) per the manufacturer's protocol. The changes in gene expression were normalized to 18S rRNA levels. A cut off Ct value of 35.0 was arbitrarily assigned such that a Ct value above 35 was considered to be undetected.

INDIRECT IMMUNOFLUORESCENCE

Cultures in two well chamber slides were washed twice in PBS and fixed with 4% paraformaldehyde (PFA, Sigma) for 20 min at room temperature followed by permeabilization with 0.2% Triton X-100 (Sigma) for nuclear markers. After washing twice with PBS, the samples were blocked with 0.1% (w/v) bovine serum albumin (BSA; Sigma) to minimize non-specific binding of antibodies. Then the samples were incubated with primary antibodies (Suppl. Table 2) overnight at 4°C and washed twice in PBS to remove non-specific binding of the primary antibody. Secondary antibody (FITC, Rhodamine) incubation was performed at room temperature for 1 h in the dark. After through washing with PBS, the cell nuclei were counterstained with 4′-6-Diamidino-2-phenylindole (DAPI, 10 μg/ml; Sigma, D9542). Cells were mounted in mounting medium (Sigma) and a glass coverslip was mounted over the chamber slides. The photographs were captured using BX-51 microscope (Olympus, UK) equipped with an Olympus DP50 digital camera (Olympus Optical Co) and analyzed using analysis® imaging software (Soft Image System GmbH).

FLOW CYTOMETRY

For fluorescence-activated cell sorting (FACS) analysis, treated and untreated cells were subjected to TrypleLE (invitrogen) treatment at 37°C to prepare single cell suspension and washed with 1× PBS. Cell suspension was fixed using 1% PFA for 1 h at room temperature. Cells were washed with wash buffer (2% serum in 1× PBS) and then incubated on ice in presence of primary antibodies albumin (Sigma) and Cytokeratin-18 (Millipore) for 1 h; again washed with wash buffer and subsequently stained with FITC-conjugated secondary antibodies along with a separate isotype control in the dark for 45 min. Finally the cell suspension was suspended in 200 μl of 1× PBS. FACS was performed on Guava EasyCyte Plus (Millipore) and data was analyzed using Cytosoft v5.2 software. A minimum of 10,000 viable cells were analyzed and the percent positivity for specific markers was calculated based on the respective isotype control.

PERIODIC ACID SCHIFF (PAS) STAINING

Cultures of differentiated cells (untreated and treated) were fixed with 10% formalin in methanol for 1 h at room temperature, and subjected to PAS staining followed by counterstaining with acidified Harris Hematoxylin according to the manufacturer's instructions (Sigma; 395B). Stained cells were observed with an inverted light microscope (Olympus).

BIOCHEMICAL ASSAYS TO ESTIMATE EXTRACELLULAR PROTEINS

The culture supernatants (spent media) from the different experimental and control groups were collected after EtOH treatment to estimate the levels of secreted proteins associated with normal development and functioning of the liver. We analyzed the levels of alpha-feto protein (AFP), serum glutamic oxaloacetic transaminase (SGOT), serum glutamic pyruvic transaminase (SGPT), and gamma-glutamyl transpeptidase (GGT). AFP was measured with Siemen's Health Care Diagnostic Kit (Cat No. 1100764) following the manufacturer's instructions using a clinical chemistry analyzer (AVIDA 1650). SGOT and SGPT were performed with Sigma Diagnostic Kits bearing catalog numbers 20764949-322 and 20764949-322 on a COBAS c501 analyzer. GGT was done using a Siemen's RxL Max Chemistry analyzer: DF 45A. All the biochemical assays were carried out in triplicates.

STATISTICAL ANALYSIS

Results were analyzed by one-way ANOVA with Tukey's multiple comparison posttests for more than two groups. Error bars on the graphs show standard deviation (SD) of at least three biological replicates ($n = 3$) or samples. Differences were considered statistically significant when $P < 0.05$ and highly significant when $P < 0.001$.

RESULTS

MORPHOLOGICAL CHANGES DURING CONVERSION OF hESCs INTO HEPATOCYTE-LIKE CELLS

hESC were initially cultured on a MEF feeder layer in the presence of fetal bovine serum and then transferred onto 1% matrigel coated plates in feeder-free conditions. Similar to feeder-dependent hESC, cells propagated in feeder-free conditions showed compact colonies with a high nuclear cytoplasmic ratio and prominent nucleoli (Fig. 1A). These cells also retained expression of key undifferentiated stem cell markers such as SSEA-4 and Oct-4 (inset of Fig. 1A). After maintaining for 4–5 days in undifferentiated state, fully-grown colonies were allowed to differentiate spontaneously by withdrawal of bFGF. During in vitro differentiation, hESCs underwent a series of profound morphological changes, most remarkable being the emergence of hepatocyte-like structures from day 7–10 onwards (Fig. 1B–D). Between days 14–21, the cells revealed typical hepatocyte morphology: Polygonal shape with distinct round nuclei (Fig. 1C–E). In the absence of HepG2-CM (control), hESCs spontaneously differentiated into a heterogeneous population of cells. Hence, this new and improvised method resulted in a substantial enrichment of hepatic progenitor cells. Interestingly, during the initial stages of differentiation at days 7–10, the non-endoderm cells were found predominantly toward the periphery of islands comprising of definitive-endoderm cells (arrows in Fig. 1B); however, with increase in the number of days in differentiation (day 14–21) these cells were outnumbered by the surging population of hepatocyte-like cells in response to HepG2-CM (Fig. 1C).

EXPRESSION OF HEPATOCYTE MARKERS IN hESC-DIFFERENTIATED CELLS

To confirm the proteomic signature of the hepatocyte-like cells observed in form of islands, we analyzed the expression profile of a set of early as well as late stage hepatocyte-specific markers including SOX-17, GATA-4, AFP, CK-18, ALB, E-Cadherin, and CYP1A2 by immunocytochemistry. The differentiated hESC treated with HepG2-CM stained positively for SOX-17, GATA-4, AFP, CK-18, ALB, E-Cadherin, and CYP1A2 (Fig. 1F–L) at day 20, whereas differentiated hESCs from the control group were weakly positive for SOX-17, GATA-4, and AFP but negative for CK-18, ALB, E-Cadherin, and CYP1A2 (data not shown). Nevertheless, some of the positively stained cells had large nuclei and polyhedral contours while others were binuclear (Fig. 1I–L). Further, we performed flow cytometric analysis to support our immunocytochemistry results. FACS analysis of differentiated hESCs at the same time point (day

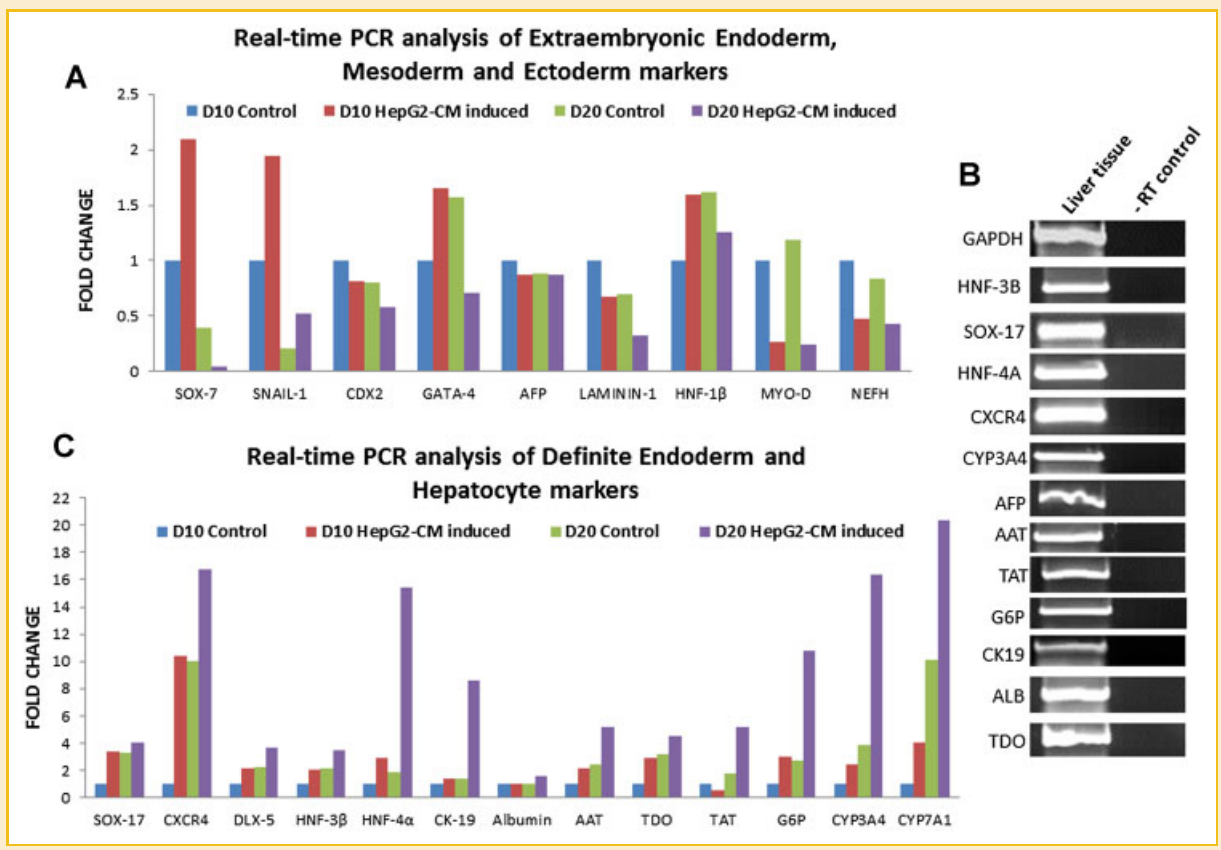

Fig. 2. Characterization of differentiated cells by gene expression profiling. A: Relative expression levels of a panel of extra embryonic, ectoderm, and mesoderm markers in the hESC-derived hepatocytes on days 10 and 20 in presence of HepG2-CM; (B) Gradual up-regulation of definitive endoderm, hepatic progenitor, and hepatocyte gene markers in induced cultures closely resembles the milestones of in vivo liver development. Stages and days in differentiation are as indicated. C: Optimization of PCR conditions for all gene markers tested was performed using total RNA from human adult liver tissue as positive control (Clontech) for RT-PCR. Genomic contamination was monitored by sample prepared without RT (−RT). Up- or down-regulation of markers was determined in relation to 18S rRNA/GAPDH gene expression used as an internal standard.

20) showed that in presence of HepG2-CM, 52, 74, 69, 85, 30, 53 and 77% of the total population were positive for GATA-4, AFP, CK-18, E-Cadherin, alpha-1-antitrypsin (AAT), albumin, and CYP7A1, respectively (Table I). In contrast, spontaneously differentiated hESCs showed very low immunoreactivity (data not shown) against these markers. This positivity toward hepatic markers may be attributed to the HepG2-CM mediated hepatic induction of HUES-7 cell line. Our data indicated significant (at least $P > 0.05$) difference in the percentage of AFP, E-Cadherin, AAT, albumin, and CYP7A1-positive cells in the hESCs differentiated in presence of HepG2-CM compared to the untreated group.

TABLE I. Represents the Percentage Positivity of Early and Late Stage Hepatocyte Markers Expressed in day 20 Harvested HepG2-CM Induced hESC Cultures Analyzed by Flow Cytometry

Serial. no	Antibody tested	Percent positive over isotype control
1	Albumin	77% ± 4.89
2	AFP	74% ± 4.24
3	CK-18	69% ± 3.91
4	E-Cadherin	85% ± 5.67
5	CYP7A1	52% ± 3.12
6	AAT	30% ± 2.18

GENE EXPRESSION PATTERN DURING IN VITRO HEPATOGENESIS SIMULATES THE STEP-WISE PROCESS OF IN VIVO LIVER DEVELOPMENT

Liver-specific gene expression was determined by quantitative real-time RT-PCR analysis at progressive stages (days 10 and 20) of hESC differentiation in presence and absence of HepG2-CM (Fig. 2A,B). In the first stage (I), spontaneously differentiating hESCs transitioned past the default pathway of extra embryonic endoderm toward definitive endoderm which was evident by clear down-regulation of extra embryonic endodermal markers including SOX-7, LAMININ-1, CDX-2, and HNF-1β (Fig. 2A). Further, it was also

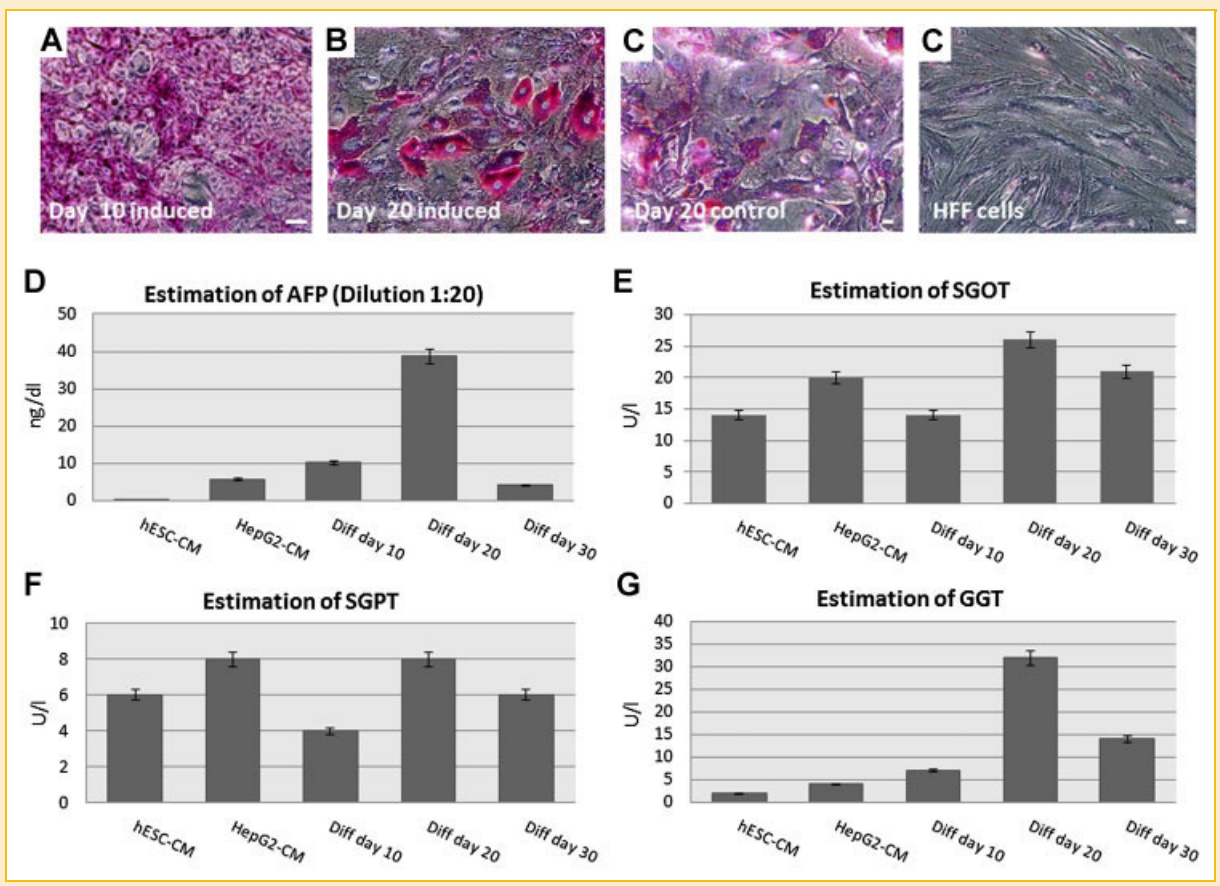

Fig. 3. Functional activity of hESC-derived hepatocytes. A–C: Cultures of hESC-derived hepatocytes (HUES-7) in presence of HepG2-CM were intensely positive for PAS staining on day 10 and 20 indicating heavy deposits of stored glycogen when compared to non-induced hESC cultures; however, (C) HFF cells (negative control) did not show positive PAS staining. Scale bar represent 100–200 μm. Biochemical analyses to determine the levels of extracellular proteins/enzymes associated with liver function. CM from day 4 undifferentiated hESC cultures and day 4 HepG2 cultures were used as controls. (D) The levels of AFP gradually increased from day 0 till day 20 in the differentiated cells; however, level of AFP produced by day 30 cultures declined indicating onset of hepatocyte-maturation. E: SGOT levels were highest in the 20-day cultures, whereas the amount of SGOT produced by day 10 and day 0 cultures was comparable. F: SGPT levels were found to be maximum again in day 20 cultures which was similar to the amount secreted by HepG2; in day 10 and day 30 cultures the protein levels were substantially lower. Both SGOT and SGPT production shows a similar trend in response to HepG2 induction. G: In case of GGT production, a sharp increase was seen from day 0 up to day 20 cultures, although more than the other time points, the GGT level suffered a significant decline on day 30. Each value represents the mean of triplicate determinations of three different cultures.

found that NEFH (neuroectoderm) and MYO-D (precardiac-mesoderm) was also down modulated in HepG2-CM induced hESCs compared to untreated control (Fig. 2A) indicating their commitment into endoderm over other lineages. The formation of definitive endoderm was confirmed by the persistent expression of SOX-17, DLX-5, CXCR4, and HNF-3β which are initially expressed by the primitive streak and continuously present in definitive endoderm progenitors (Fig. 2B). Following addition of HepG2-CM at stage II of the protocol, markers associated with hepatic progenitors like HNF-4α, AFP, and CK-19 were enhanced (Fig. 2B). Lastly at stage III, expression of albumin, the most abundant protein in the liver was significantly elevated (Fig. 2B). AFP and CK-19 are expressed in cytoplasm during the differentiation of the fetal liver. Other proteins related to liver functions were also found to be substantially up-regulated at this stage, such as tyrosine transferase (TAT), AAT, glucose 6-phosphate (G6P), tryptophan-2, 3-dioxygenase (TDO), cytochrome P450 subunit 3a4 and 7a1 (CYP3A4 and CYP7A1) (Fig. 2B). Expectedly, hESC grown in absence of HepG2-CM demonstrated low or very low levels of these hepatocyte-specific genes; furthermore, markers of stemness such as of Oct-4, Nanog, and SOX-2 were found to be down-regulated over the course of differentiation (data not shown). The data on optimization of PCR conditions and the specificity of all hepatocyte markers tested in this study (Suppl. Table 1) are shown in Figure 3C using total RNA from human liver (Clontech) as positive control.

FUNCTIONAL ACTIVITY OF hESC-DERIVED HEPATOCYTE-LIKE CELLS

Since human hepatocytes can make and store glycogen, we analyzed glycogen levels by six PAS staining. The number of cells positively stained in the HepG2-CM treated cultures at day 10 and day 20 was higher than non-induced cultures (Fig. 3A–C). HFF were used as negative control for PAS staining (Fig. 3D). For the ELISA/ECLIA-based biochemical assays, we compared the levels of extracellular

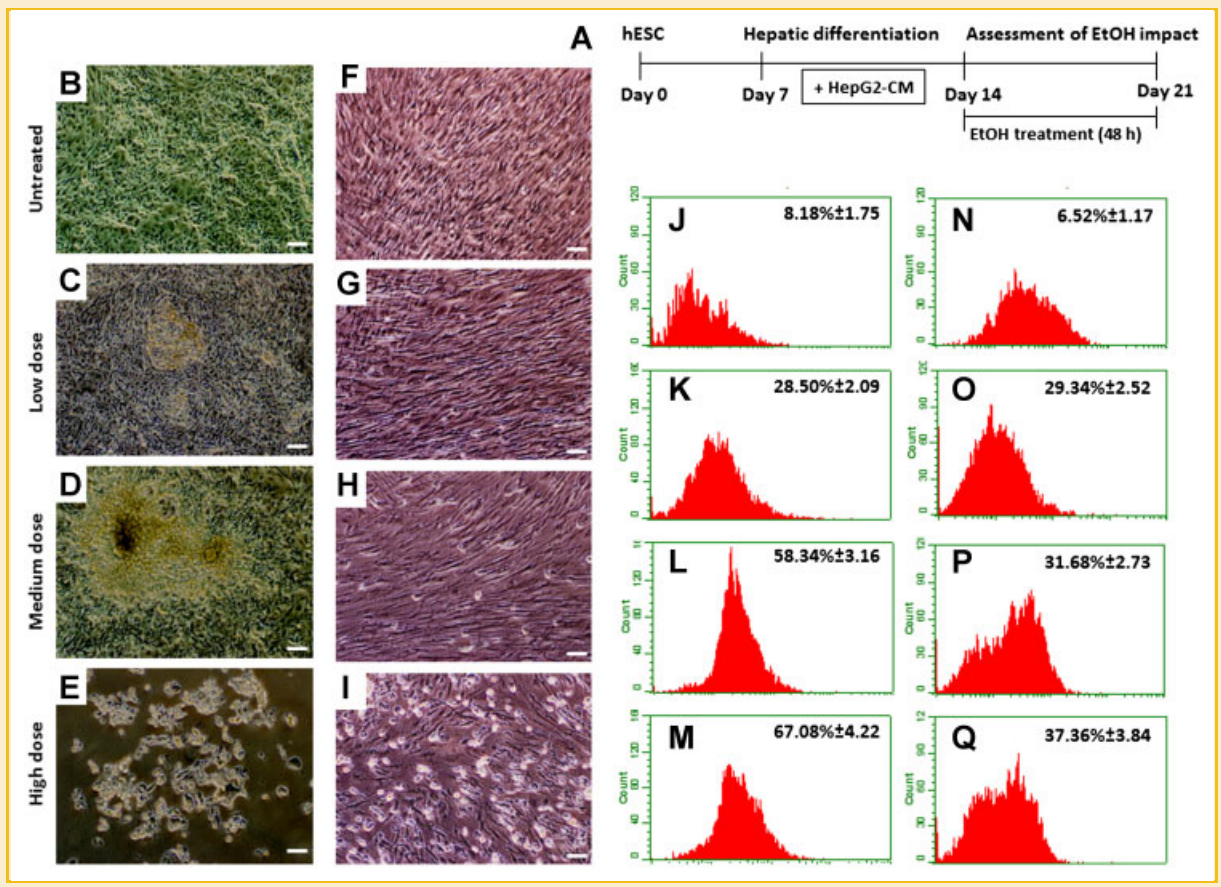

Fig. 4. Impact of EtOH on morphology and viability of hepatocyte-like cells. A: A schematic presentation of the experimental set up to examine the effects of alcohol on HepG2-CM induced hESC cultures. B–E: Differentiating hESC (HUES-7) cultures at day 20 were exposed to EtOH at concentrations of 50 (high dose), 20 (medium dose), 5 (low dose), and 0 mM (untreated control), respectively. Concentrations of 50 mM induced abnormalities in cell morphology and loss of cellular attachment; 20 mM caused shrinking and blackening of cells while 5 mM produced a more stable and viable phenotype when compared to untreated cultures. F–I: Similarly, 50 mM EtOH produced distortion of fibroblastic-morphology and detachment of HFF cells; however, 20 and 5 mM concentrations produced little or no changes in the HFF. Representative data from one of three experiments are shown. Scale bar: 100 μm. E–H: Effect on cell survival at day 20 under different experimental conditions was evaluated by calculating the percentage of cells positive for the cell-impermeant DNA fluorophore 7-AAD. J–M: Quantification of the results was performed by flow cytometry; 20 and 50 mM EtOH caused a remarkable reduction in the cell viability. N–Q: Likewise, viability of HFF suffered a dose dependent decrease in response to EtOH exposure. Values are presented as means ± SD (n = 3).

liver-specific proteins like AFP, SGOT, SGPT, and GGT secreted in the spent media of undifferentiated hESC and HepG2 (only) cultures with that of HepG2-CM treated hESC cultures at days 10, 20, and 30 (Fig. 3E–H). AFP is known as an endodermal and a fetal liver marker. Although undifferentiated hESC did not secrete any AFP, hepatocyte-like cells produced maximum level of AFP at day 20 (38.6 ng/dl), which was significantly higher than that of HepG2 cells alone (Fig. 3D). Further, the AFP levels declined remarkably on day 30 indicating maturation of hepatocytes. In our study, we detected highest levels of both SGOT (26 U/L) and SGPT (8 U/L) in the day 20 HepG2-CM treated cultures (Fig. 3E,F). However, conditioned media collected from HepG2 cultures (only) also showed relatively enhanced levels of both the enzymes compared to undifferentiated hESC and day 10 HepG2-CM treated cells (Fig. 3E,F). We found a gradual increase of GGT activity from undifferentiated hESCs to HepG2-CM induced hepatocyte-like cells (Fig. 3G). Interestingly, the GGT levels peaked to 32 U/L in day 20 compared to the controls and also the day 30 cultures (Fig. 3G); however, the results of all the test samples were well within the normal range GGT levels (40–80 U/L) found in blood serum.

DOSE AND STAGE DEPENDENT ACTION OF EtOH ON MORPHOLOGY AND CELL SURVIVAL OF HEPATIC PROGENITORS

We exposed differentiated hESCs at day 20 to EtOH concentrations of 0, 5, 20, and 50 mM for 48 h (Fig. 4B–E); we used HFF as an independent control for the cytotoxicity studies (Fig. 4F–I). Cells exposed to 50 mM EtOH and greater suffered permanent phenotypic changes with respect to individual cell shape, epithelial morphology, and complete loss of attachment (Fig. 4E). Although cultures exposed to 5 mM showed some phenotypic changes in cellular morphology, they were least affected by EtOH and appeared most likely to endure experimentation (Fig. 4B,C). Based on these observations we used 20 mM as the preferred concentration to study the effects of alcohol toxicity; further, 20 mM EtOH equates to a blood alcohol concentration (BAC) of 0.10% which is physiologically relevant. Hence, we showed that exposure of hESC cultures to doses of EtOH reflecting casual drinking can be used as an in vitro model to understand alcohol-mediated cytoxicity.

We then examined the effect of EtOH on cell survival. Flow cytometry analysis revealed that EtOH treatment significantly escalated the 7-AAD positive population. Moreover, the data in Figure 4 also demonstrate that while 5 mM EtOH is able to induce cell death witnessed by increase in 7-AAD positivity, higher concentrations of EtOH, such as 20 and 50 mM triggers necrotic cell death as evident by a drastic increase in 7-AAD positive population (Fig. 4J–M). Although a similar pattern of cell mortality was observed in control HFFs, the percentage of cell death due to EtOH toxicity was relatively low in response to the 20 and 50 mM concentrations (Fig. 4N–Q). It was evident that EtOH treatment selectively affected the HepG2-CM induced hESC cultures when compared to the spontaneously differentiating hESC (data not shown). Taken together these results suggest that EtOH insult causes a massive decline in cell viability probably by aggravation of apoptotic as well as necrotic cell death.

EtOH AFFECTS THE EXPRESSION OF HEPATOCYTE MARKERS AND PERTURBS THE IN VITRO DEVELOPMENTAL PROGRAM

In hESCs, differentiation is determined by a series of genetic and proteomic changes. To gain additional insight into the potential actions and mechanisms of EtOH on the hESC-derived hepatocyte-like cells during in vitro proliferation, differentiation, and maturation we evaluated the expression levels of a candidate set of gene markers by semi-quantitative RT-PCR analysis on day 20 cultures. While the levels of the undifferentiated stem cells transcription factors like Rex1 and Oct-4 were reduced in a dose dependent fashion, EtOH treatment did not affect Nanog expression (Fig. 5A). As the spotlight of this study is to understand liver toxicity, most interestingly we found that EtOH treatment significantly upsets the expression of marker genes associated with the formation of definitive endoderm, hepatic progenitors, and functional hepatocytes. While HNF-3β, SOX-17, and GATA-6 levels demonstrated a distinct down-regulation in a dose-dependent manner at day 20, expression of GATA-4 was unchanged in the LD (5 mM) but was completely obliterated in the MD (20 mM) and HD (50 mM) of EtOH compared to the untreated control (Fig. 5A). Furthermore, a distinct decrease in the expression levels of HNF-4α, CK-18, TDO, albumin, G6P and CYP3A4 was observed particularly in response to 50 mM of EtOH (Fig. 5A), but was not much significant in 20 and 5 mM concentrations.

To lend support to the gene expression profiling, we performed flow cytometry and imunocytochemical analyses of differentiating hESCs on day 20. FACS studies revealed a drastic reduction in the percentage of CK-18 (Fig. 5B–E) and albumin (Fig. 5F–I) positive cells in EtOH treated cultures compared to that of the untreated control groups. However, HFF was found to be more resistant to EtOH treatment than hESCs perhaps because of their fibroblastic nature. day 20 EtOH exposure strikingly affected the cellular morphology and structural integrity of hepatocyte-like cells. Figure 6A–D shows how EtOH alters the morphological characteristics and localization pattern of albumin staining and decreases the number of cells stained. Furthermore, a noticeable effect of EtOH-induced toxicity was considerable disruption in the cellular architecture and cytoskeleton in the MD (20 mM) and HD (50 mM) (Fig. 5D,E); however, barely any impact was detectable in the LD (5 mM) group neither in immunocytochemistry nor FACS (Fig. 5C,G).

EtOH INHIBITS HEPATIC MATURATION AND LIVER FUNCTION

To confirm the above findings we performed two separate assays to determine whether EtOH alters the glycogen storage and AFP production capacity in the HepG2-CM induced cultures in comparison to HepG2 cultures (only) and untreated hESC. We found that the number of cells positive for PAS staining decreased drastically after EtOH treatment especially in the 20 and 50 mM concentrations (Fig. 6E–H) which indicates loss of glycogen deposits in the putative hepatocytes. AFP is a major plasma protein produced by the yolk sac and the liver during fetal life and is also considered to be the fetal counterpart of serum albumin. Biochemical analysis of the spent media collected from EtOH exposed hESC cultures showed significant decline in AFP levels in a dose dependent manner (Fig. 6I). Given that the normal range of AFP in adults is reported as

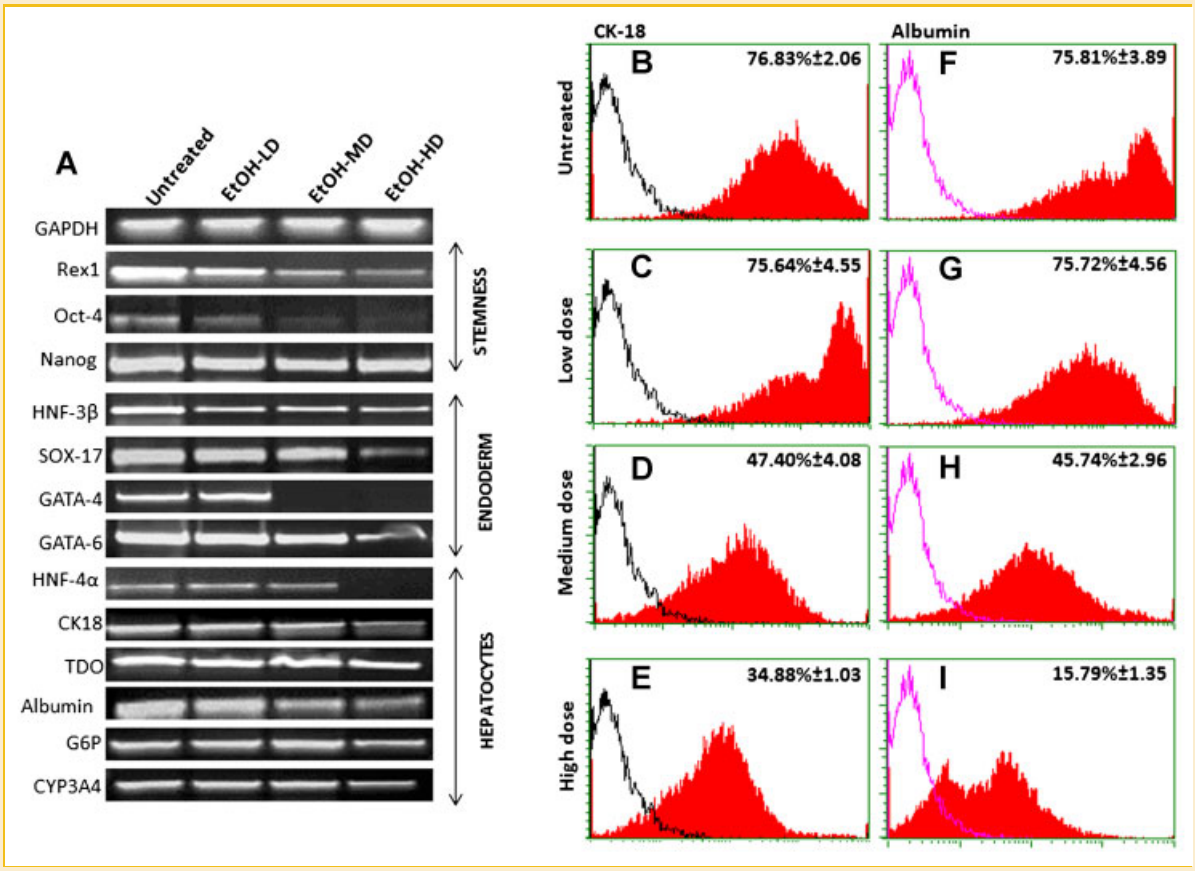

Fig. 5. EtOH exposure alters the molecular and proteomic characteristics of hepatocyte-like cells. A: Semi quantitative RT-PCR analysis demonstrates down-regulation of a candidate set of genes associated with stemness and liver-specific gene markers. The adverse impact of EtOH on the transcriptional signature of the cells at day 20 was clearly dose-dependent when compared with untreated hESC as positive control. B–I: Immunophenotyping by flow cytometry confirms the adverse effect of EtOH treatment. B–E: The percentage of cells positive for CK-18 shows a gradual decline in EtOH treated groups in a dose dependent manner; (F–I) Likewise, the percent positivity against albumin antibody falls drastically in the highest dose (50 mM) of EtOH; 20 mM also causes a substantial decrease in albumin immunoreactivity very little or no significant change was observed in the 5 mM concentration. Values are presented as means ± SD (n = 3).

under 50 ng/ml, our results were clinically relevant. Moreover, the amount of extracellular AFP detected in the HepG2-CM induced day 20 hESC was much higher (Fig. 4D) when compared with that of EtOH treated hESC on the same time point (Fig. 6I) which is a direct evidence of EtOH-induced toxicity. All these results showing multiple facets of abnormal liver function may be attributed to EtOH mediated damage inflicted on in vitro hepatocytes.

DISCUSSION

The purpose of the present investigation is twofold; first, to generate functional hepatocytes from hESCs following a simple protocol using CM from a hepatocarcinoma cell line HepG2 and second, to determine the influence of EtOH exposure on hepatic induction, differentiation, and maturation. In response to HepG2-CM induction, we witnessed the morphological changes in cellular architecture of hESCs from tightly packed colonies to islands of epithelial-like cells followed by their gradual conversion into polygonal cells with multiple nuclei in a span of 2–3 weeks. This phenotypic transition of undifferentiated cells toward differentiated hepatocytes was accompanied by the appearance of stage-specific transcription factors, structural proteins, and cytoplasm loaded with glycogen granules (Fig. 1F–L; Fig. 3A–C). The true epithelial nature of these putative hepatocytes was supported by the localization of CK-18 and E-cadherin. The sequential expression of genes along the hepatocyte differentiation pathway was demonstrated; initiated by up-regulation of markers responsible for definitive endoderm followed by hepatic progenitors and mature hepatocyte-specific markers (Fig. 2B). This was also accompanied by the down-regulation of extra embryonic endoderm, ectoderm, and mesoderm markers in HepG2-CM induced hESC versus spontaneously differentiating hESC confirming their definitive endodermal origin (Fig. 2A). It is also evident (Fig. 3E–H) that these newly formed hepatocyte-like cells exhibited multiple liver functions.

We hypothesized that the differentiation efficiency of hESC can be improved if proper signals are provided to the uncommitted hESCs at the best level of their competence to differentiate into the destined phenotype. It has been shown earlier that HepG2-CM, obtained from liver carcinoma cells with characteristics similar to

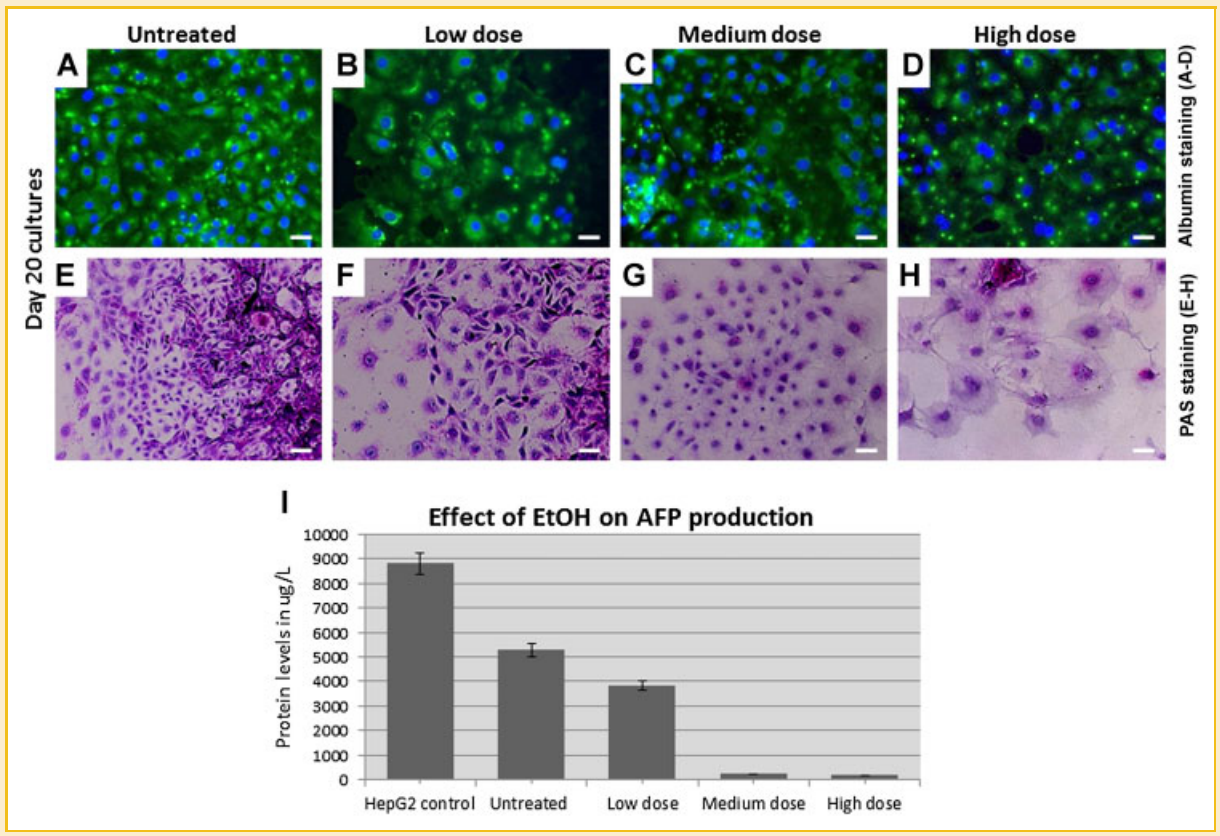

Fig. 6. Impairment in functional activity of hepatocytes as a result of EtOH insult. A–D: Immunocytochemical staining establishing the deleterious impact of EtOH treatment; in addition to reduction in the number of albumin positive cells, higher concentrations like 20 and 50 mM produced extensive nuclear disintegration and cytoskeletal disruption. Representative data from one of three experiments are shown. E–H: EtOH exposure leads to reduction in the number and intensity of PAS staining in hepatocyte-like cells in a dose dependent manner implicating diminution of glycogen deposits which is an important attribute of functional hepatocytes. Fifty millimolar EtOH also produced massive distortion in the epithelial architecture and polygonal morphology of the cells thereby giving rise to stress fibers. Scale bar: 100 μm. I: Examination of extracellular AFP levels in supernatants collected from hESCs demonstrated a gradual and significant decline with an increase in EtOH concentration. Since HepG2 is a hepatocarcinoma cell line, the levels of AFP was relatively higher in the HepG2-CM (only) group. All data is representative of three separate experiments ($n = 3$) and was in concurrence with the standard levels of corresponding proteins in human serum.

visceral endoderm (VE), resulted in enhanced mesoderm formation from murine ESCs [Hwang et al., 2006]. Furthermore, Rathjen et al. guided lineage-specific differentiation of mESCs towards nascent mesoderm [Rathjen et al., 2003] and neuroectoderm [Rathjen et al., 2002] by using HepG2-CM. These reports draw support from the long-standing concept that VE acts as an early organizer, which secretes signaling molecules that specify cell fate during embryogenesis [Bielinska et al., 1999]. In our study, hESCs treated with HepG2-CM were converted to cells resembling those in the definitive endoderm followed by their transformation into hepatocyte-like cells. However non-hepatic and hepatic cells in the cultures were morphologically different and could be easily distinguished under bright field microscopy. Recently proteomic analysis of HepG2-CM has revealed the presence of trophic factors which might be responsible for the inductive effect toward liver formation [Kang et al., 2009]. This evidence explains the possible role of heterotypic paracrine–juxtacrine interactions underlying the inductive effect of HepG2 in formation of functional hepatocytes. Furthermore, the time point at which HepG2-CM was collected is crucial because maximum level of extracellular (paracrine) secretions is directly proportional to the functional status of the cells in culture. We chose and treated the hESC cultures with HepG2-CM collected on day 3–4 (stationary phase) and obtained maximum efficacy of hepatocyte induction on day 20. Taken together, the first part of our study highlights the possibility of employing biological preconditioning as the source of "*instructive*" signals for liver-specific differentiation of hESC. We envisage that this in vitro model may be useful in future investigations to elucidate the molecular mechanisms governing hepatocyte differentiation and liver development.

Although liver damage caused by ALD is reversible when diagnosed at the earlier stages, current risk assessment tools are relatively non-specific. Hence identification of an early specific signature of ALD would aid in therapeutic intervention and recovery. We showed that EtOH treatment prompted disruption of characteristic hepatocyte morphology of the cells (Fig. 4B–E) thereby leading to increased mortality (Fig. 4J–M) followed by down-regulation of liver-specific markers (Fig. 5A–I; Fig. 6A–D) and subsequent decline in the levels of stored glycogen and AFP (Fig. 6E–I). This dose-dependent effect of EtOH on the progressive stages of hepatocyte formation simulates the in vivo situation of

alcohol exposure during early pregnancy. Our findings suggest that there is a selective impact of EtOH on the differentiated or committed cells compared to undifferentiated stem cells or fibroblasts. Interestingly 5 mM EtOH does not seem to affect the mRNA transcript levels of stemness- or lineage-specific genes; on the other hand 20 and 50 mM EtOH showed an irreversible and detrimental effect with respect to all the parameters that we tested. Therefore, we deemed 20 mM EtOH as the cut off limit for our study; furthermore, this concentration equates to a BAC of 0.10%. This level of BAC can be obtained through casual drinking and does not emulate BAC of alcoholics, which can reach as high as 0.50% or greater. Both medium (20 mM) and high concentrations (50 mM) of EtOH produced a significant decrease in the expression of undifferentiated stem cell markers namely Oct-4 and Rex1 in a dose dependent fashion indicating the onset of premature differentiation resulting in abnormal development (Fig. 5A). Most importantly, EtOH treatment affected the levels of early as well as late-stage liver markers; HNF-3β, HNF-4α, SOX-17, GATA-4, ALB, CK-18, and CYP3A4 were markedly down-regulated in the 20 and 50 mM concentrations of EtOH (Fig. 5A). These molecular data were well supported by our proteomic data wherein we observed a substantial reduction in the percentage of cells positive for CK-18 (Fig. 5B–E) and albumin (Fig. 5F–I) in the cultures treated with 20 and 50 mM EtOH. In all, the data showing deterioration of hepatocyte-like cells in response to 48 h of EtOH exposure may be corroborated with chronic liver damage produced by casual or binge drinking. This conclusion draws support from the strong clinical evidence showing maternal alcohol consumption causing delayed and abnormal fetal development [Robinson et al., 2010]. On a whole, alcohol-induced imbalance in the hESC differentiation pathway provides new information that may be valuable for deciphering mechanisms involved in the genesis of FASD.

Further, the depletion in glycogen depot (reserve) upon EtOH exposure is in concurrence with alcohol-induced glycogenolysis. Again, the drastic reduction in AFP production suggests untimely maturation of newly generated hepatic progenitors at day 20 (Fig. 6I). Oxidative stress and inflammation are two major etiological factors that play key roles in the development of EtOH induced liver injury. Release of proinflammatory cytokine like tumor necrosis factor alpha (TNF-α) and activation of nuclear factor kappa-B (NFκ-B) may strongly intensify inflammation and cell damage. Therefore, we hypothesized that these features of the effect of alcohol could be hazardous to normal hepatocyte turn over in the adult liver leading to liver cirrhosis.

In nutshell, our study demonstrates adverse effects of alcohol on liver formation with respect to down-regulation of gene and protein markers, increase of cell mortality leading to disruption of typical hepatocyte architecture, and functional activity hepatocyte-like cells. We documented for the first time that almost all the facets of liver damage due to alcohol exposure can be modeled in vitro employing hESC-based platform. Our system is thus unique and different from all other existing in vitro models for hepatotixicity screening as it is less complicated, cost-effective, quick, and not so tedious. However, detailed knowledge of the specific signaling molecules present in the HepG2-CM is still limited and hence warrants further exploration. In addition, the use of the CM, especially for potential clinical applications, suffers from the risk for transmission of pathogens and also variability in quality depending on the cell's physiological status.

ACKNOWLEDGMENTS

The work was supported by Stempeutics Research Malaysia. The authors are grateful to Ms Saratha Devi Thrichelvam for technical help in flow cytometry and Dr. Vijay Bhat, Biochemistry Department, Manipal Hospital, Bangalore for performing some of the biochemical assays. They also thank Dr. Mahendra Rao, Center for Regenerative Medicine, NIH, Bethesda, Maryland for critical review of the manuscript and valuable suggestions.

REFERENCES

Baroni GS, Marucci L, Benedetti A, Mancini R, Jezequel AM, Orlandi F. 1994. Chronic ethanol feeding increases apoptosis and cell proliferation in rat liver. J Hepatol 20(4):508–513.

Barr HM, Streissguth AP. 2001. Identifying maternal self-reported alcohol use associated with fetal alcohol spectrum disorders. Alcohol Clin Exp Res 25(2):283–287.

Basma H, Soto-Gutierrez A, Yannam GR, Liu L, Ito R, Yamamoto T, Ellis E, Carson SD, Sato S, Chen Y, Muirhead D, Navarro-Alvarez N, Wong RJ, Roy-Chowdhury J, Platt JL, Mercer DF, Miller JD, Strom SC, Kobayashi N, Fox IJ. 2009. Differentiation and transplantation of human embryonic stem cell-derived hepatocytes. Gastroenterology 136(3):990–999.

Bielinska M, Narita N, Wilson DB. 1999. Distinct roles for visceral endoderm during embryonic mouse development. Int J Dev Biol 43(3):183–205.

Brolen G, Sivertsson L, Bjorquist P, Eriksson G, Ek M, Semb H, Johansson I, Andersson TB, Ingelman-Sundberg M, Heins N. 2010. Hepatocyte-like cells derived from human embryonic stem cells specifically via definitive endoderm and a progenitor stage. J Biotechnol 145(3):284–294.

Cai J, Zhao Y, Liu Y, Ye F, Song Z, Qin H, Meng S, Chen Y, Zhou R, Song X, Guo Y, Ding M, Deng H. 2007. Directed differentiation of human embryonic stem cells into functional hepatic cells. Hepatology 45(5): 1229–1239.

Cartwrigh MM, Tessmer LL, Smith SM. 1998. Ethanol-induced neural crest apoptosis is coincident with their endogenous death, but is mechanistically distinct. Alcohol Clin Exp Res 22(1):142–149.

Duan Y, Catana A, Meng Y, Yamamoto N, He S, Gupta S, Gambir SS, Zern MA. 2007. Differentiation and enrichment of hepatocyte-like cells from human embryonic stem cells in vitro and in vivo. Stem Cells 25(12): 3058–3068.

Dunty WC Jr, Chen SY, Zucker RM, Dehart DB, Sulik KK. 2001. Selective vulnerability of embryonic cell populations to ethanol-induced apoptosis: Implications for alcohol-related birth defects and neurodevelopmental disorder. Alcohol Clin Exp Res 25(10):1523–1535.

Elaut G, Papeleu P, Vinken M, Henkens T, Snykers S, Vanhaecke T, Rogiers V. 2006. Hepatocytes in suspension. Methods Mol Biol 320:255–263.

Greer ML, Barber J, Eakins J, Kenna JG. 2010. Cell based approaches for evaluation of drug-induced liver injury. Toxicology 268(3):125–131.

Gualdi R, Bossard P, Zheng M, Hamada Y, Coleman JR, Zaret KS. 1996. Hepatic specification of the gut endoderm in vitro: Cell signaling and transcriptional control. Genes Dev 10(13):1670–1682.

Guan Z, Lui CY, Morkin E, Bahl JJ. 2004. Oxidative stress and apoptosis in cardiomyocyte induced by high-dose alcohol. J Cardiovasc Pharmacol 44(6):696–702.

Guillouzo A, Corlu A, Aninat C, Glaise D, Morel F, Guguen-Guillouzo C. 2007. The human hepatoma HepaRG cells: A highly differentiated model for

studies of liver metabolism and toxicity of xenobiotics. Chem Biol Interact 168(1):66–73.

Hay DC, Fletcher J, Payne C, Terrace JD, Gallagher RC, Snoeys J, Black JR, Wojtacha D, Samuel K, Hannoun Z, Pryde A, Filippi C, Currie IS, Forbes SJ, Ross JA, Newsome PN, Iredale JP. 2008. Highly efficient differentiation of hESCs to functional hepatic endoderm requires Activin A and Wnt3a signaling. Proc Natl Acad Sci USA 105(34):12301–12306.

Hay DC, Zhao D, Fletcher J, Zoe A, Hewitt A, Mclean D, Urruticoechea-Uriguen A, Black JR, Elcombe C, Ross JA, Wolf R, Cui W. 2008. Efficient differentiation of hepatocytes from human embryonic stem cells exhibiting markers recapitulating liver development in vivo. Stem Cells 26:894–902.

Hwang YS, Randle WL, Bielby RC, Polak JM, Mantalaris A. 2006. Enhanced derivation of osteogenic cells from murine embryonic stem cells after treatment with HepG2-conditioned medium and modulation of the embryoid body formation period: Application to skeletal tissue engineering. Tissue Eng 12(6):1381–1392.

Kang Y, Nagy JM, Polak JM, Mantalaris A. 2009. Proteomic characterization of the conditioned media produced by the visceral endoderm-like cell lines HepG2 and END2: Toward a defined medium for the osteogenic/chondrogenic differentiation of embryonic stem cells. Stem Cells Dev 18(1):77–91.

Li Z, Lin H, Zhu Y, Wang M, Luo J. 2001. Disruption of cell cycle kinetics and cyclin-dependent kinase system by ethanol in cultured cerebellar granule progenitors. Brain Res 132(1):47–58.

Manna SK, Patterson AD, Yang Q, Krausz KW, Li H, Idle JR, Fornace AJ, Jr., Gonzalez FJ. 2010. Identification of noninvasive biomarkers for alcohol-induced liver disease using urinary metabolomics and the Ppara-null mouse. J Proteome Res 9(8):4176–4188.

Miller MW, Chiaia NL, Rhoades RW. 1990. Intracellular recording and injection study of corticospinal neurons in the rat somatosensory cortex: Effect of prenatal exposure to ethanol. J Comp Neurol 297(1):91–105.

Rambhatla L, Chiu CP, Kundu P, Peng Y, Carpenter MK. 2003. Generation of hepatocyte-like cells from human embryonic stem cells. Cell Transplant 12(1):1–11.

Rathjen J, Haines BP, Hudson KM, Nesci A, Dunn S, Rathjen PD. 2002. Directed differentiation of pluripotent cells to neural lineages: Homogeneous formation and differentiation of a neurectoderm population. Development 129(11):2649–2661.

Rathjen J, Washington JM, Bettess MD, Rathjen PD. 2003. Identification of a biological activity that supports maintenance and proliferation of pluripotent cells from the primitive ectoderm of the mouse. Biol Reprod 69(6):1863–1871.

Robinson M, Oddy WH, McLean NJ, Jacoby P, Pennell CE, de Klerk NH, Zubrick SR, Stanley FJ, Newnham JP. 2010. Low-moderate prenatal alcohol exposure and risk to child behavioural development: A prospective cohort study. BJOG 117(9):1139–1150.

Schwartz RE, Linehan JL, Painschab MS, Hu WS, Verfaillie CM, Kaufman DS. 2005. Defined conditions for development of functional hepatic cells from human embryonic stem cells. Stem Cells Dev 14(6):643–655.

Shirahashi H, Wu J, Yamamoto N, Catana A, Wege H, Wager B, Okita K, Zern MA. 2004. Differentiation of human and mouse embryonic stem cells along a hepatocyte lineage. Cell Transplant 13(3):197–211.

Siegenthaler JA, Miller MW. 2004. Transforming growth factor beta1 modulates cell migration in rat cortex: Effects of ethanol. Cereb Cortex 14(7):791–802.

Tuschl G, Lauer B, Mueller SO. 2008. Primary hepatocytes as a model to analyze species-specific toxicity and drug metabolism. Expert Opin Drug Metab Toxicol 4(7):855–870.

Young C, Klocke BJ, Tenkova T, Choi J, Labruyere J, Qin YQ. 2003. Ethanol-induced neuronal apoptosis in vivo requires BAX in the developing mouse brain. Cell Death Differ 10(10):1148–1155.

Zaret KS, Watts J, Xu J, Wandzioch E, Smale ST, Sekiya T. 2008. Pioneer factors, genetic competence, and inductive signaling: Programming liver and pancreas progenitors from the endoderm. Cold Spring Harb Symp Quant Biol 73:119–126.

Zorn AM, Wells JM. 2009. Vertebrate endoderm development and organ formation. Annu Rev Cell Dev Biol 25:221–251.